

RESEARCH NOTE

H₂O Splitting in Tubular Plasma Reactors

Xiao Chen,^{*} Manuel Marquez,^{*§} Jeff Rozak,[†] Carolina Marun,[†] Jian Luo,^{*} Steven L. Suib,^{*,†,‡,1}
Yuji Hayashi,[†] and Hiroshige Matsumoto^{*}

^{*}*U-60, Department of Chemistry, †Department of Chemical Engineering, ‡Institute of Materials Science, University of Connecticut, Storrs, Connecticut 06269; and §Department of Applied Physics and Electrical Engineering, Yale University, New Haven, Connecticut 06511*

Received September 2, 1997; revised March 23, 1998; accepted April 27, 1998

Significant hydrogen productivity (0.33 mol% in products) from H₂O splitting by atmospheric dielectric barrier discharges has been achieved with tubular plasma reactors at room temperature. The water splitting activity varies with different metal-coated inner electrodes and different peak voltages across the reactor. An optimal emission spectroscopic study was performed in order to explain the metal effect. O^{*}/Ar^{*} emission intensity ratio as well as excitation temperatures were used for rationalizing the metal effect. © 1998

Academic Press

I. INTRODUCTION

The predicted exhaustion of limited and unevenly distributed world fossil fuel reserves in the middle of the 21st century has focused attention on water splitting technologies to produce hydrogen which is a clean, renewable, and nonpolluting fuel and an energy carrier from an unlimited source (1). Czuppon *et al.* presented an excellent review on different water splitting techniques, such as electrochemical water splitting (electrolysis), one-step or multistep thermochemical water splitting, and water splitting with solar energy (2). Amouyal (3), Bolton (4), and Bard *et al.* (5) published reviews on splitting of water to hydrogen and oxygen via solar energy. These different water splitting techniques are still in development and only the electrolysis method is in industrial use to a limited extent, due to the low overall efficiency of 20–35% (2).

Nonequilibrium cold plasmas have been considered as highly efficient ways to use electrical energy to excite gaseous reactants and several technological applications in chemical processes have been summarized by Badyal (6). Applications of plasmas in catalyst preparation and catalytic reactions have been recently reviewed by Kizling and Järås (7). The silent discharge, a kind of nonequilibrium cold plasma also known as an atmospheric dielectric barrier

discharge, is ideal for dissociating molecules which are very difficult to be decomposed thermodynamically, such as ammonia, hydrogen sulfide, methane, and water, as suggested by Fridman and Rusanov (8). Many studies have been done with ammonia (9–11), hydrogen sulfide (11), and methane (12, 13), but we are not aware of studies of water splitting with plasmas.

II. EXPERIMENTAL SECTION

A. Plasma Reactors

Recently, we have studied water splitting with atmospheric dielectric barrier discharges in a tubular reactor using plasma and catalyst integrated technologies (PACT) (14). A schematic diagram of the tubular PACT reactor is shown in Fig. 1. The basic principle of the reactor involves an inner metal-coated electrode which is used as a catalyst for activation of the reactants. The atmospheric dielectric barrier discharge between the inner electrode and the part of the quartz tube that covers the outer electrode produces a plasma zone for excitation of molecules when a high alternating current (AC) is applied to both electrodes. Synergistic effects of catalytic activation and plasma excitation are expected to exist in this reactor.

Tubular PACT reactors with metal (either Ni, Pd, Rh, or Au) coated inner electrodes (M-tubular PACT reactors) and outer electrodes made of aluminum foil were used in our experiments at room temperature and atmospheric pressure. Feed compositions were 2.3 mol% of H₂O with a balance of argon and a total flow rate of 10 mL/min at 1 atm. The circuit diagram for the tubular PACT reactor is shown in Fig. 2.

The water concentration was determined from the partial pressure of water vapor in a bubbler at room temperature assuming that argon is saturated by water vapor after passing through the bubbler. This assumption has been confirmed by measurements of the weight of water collected in a cold trap after the bubbler.

¹ To whom correspondence should be addressed.

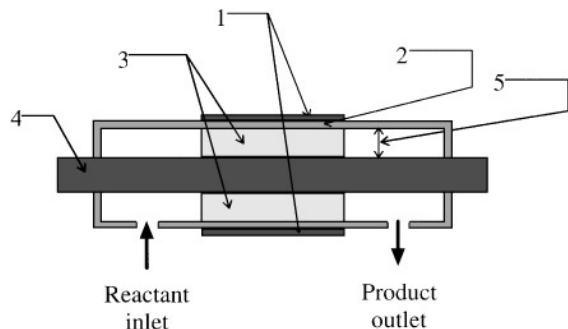


FIG. 1. Schematic diagram of the cross section of a tubular PACT reactor: 1. outer electrode; 2. quartz tube; 3. glow discharge zone; 4. inner electrode; 5. discharge gap.

B. Plasma Reactions

The reaction was started by applying a high alternating current produced by a UHV-10 type high frequency (8.1 kHz) AC power supply (made by Nihon Inter Electronics Corporation, Japan). The output voltage of the power supply can be increased directly by increasing its voltage dial setting. The AC voltage waveforms between the inner and outer electrodes in the reactor were recorded with a Yokogawa (Yokogawa Electric Corporation, Japan) DL 1540 digital oscilloscope during reaction via a Tektronix P6025A high voltage probe. The peak value of the AC voltage waveform is defined as the peak voltage (V_p). The input voltage $V_{in(p-p)}$ (peak to peak value on the AC input voltage trace) for the reactor was recorded when the reactor is disconnected with the dial setting on the UHV-10 type high frequency (8.1 kHz) power supply at the value to be used in experiments. The gap current (i) through the inner and outer electrodes was calculated after measuring the voltage of a standard resistor (100 Ω) with the DL 1540 digital oscilloscope with a Yokogawa 70996 voltage probe. The voltage across and current through the reactor were recorded as a function of time with the Yokogawa DL 1540 digital oscilloscope. The power consumed by the reactor was determined

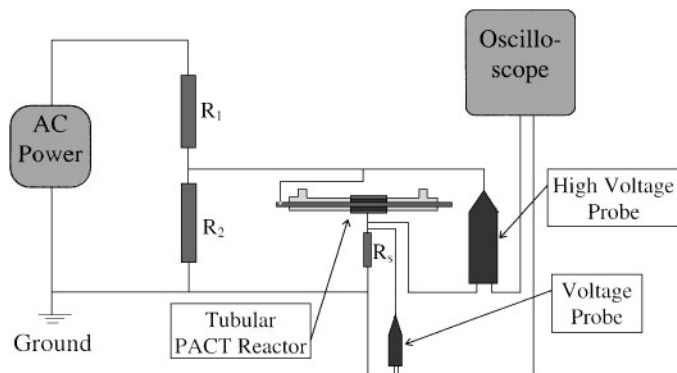


FIG. 2. Circuit diagram for the tubular PACT reactor: $R_1 = 50$ kW; $R_2 = 100$ kW; $R_3 = 100$ W.

by integrating the product of the current and voltage as a function of time and dividing it by the total time period.

C. Chemical Analysis

The outlet gases from the reactor were analyzed on-line with a Hewlett Packard 5890 Series II gas chromatograph (GC) equipped with a Carboxen-1000 (45/60 mesh) column and a thermal conductivity detector. The formation of hydrogen and oxygen in the products was observed with GC methods at levels of 0.2 and 0.1 mol%, respectively.

D. Optical Emission Spectroscopy Study

Optical emission spectroscopy (OES) was used to understand the unique role the metal plays in water splitting. OES studies were carried out in the 200–900 nm range using a 270M Spex instrument with a liquid nitrogen-cooled CCD detector. Light emitted from the plasma is collected and directed to a monochromator with a fiber optic cable. The accuracy of the position of the emission lines in the spectra is 0.1 nm. The helium and argon used for these studies were 99.99% pure.

An aluminum jacket with a series of holes was used to collect the light emitted from different plasma regions. Argon and helium emission spectra were collected first in two different set of experiments: (a) with a constant input voltage for different metals in order to observe emission changes due to metal effects and (b) with the same metal and different input voltage (V_i) to measure the V_i effect on the distribution of the excited states.

III. RESULTS AND DISCUSSIONS

A. Plasma Reactions

Figure 3 shows experimental results for H₂O splitting in the tubular PACT reactors with different metal-coated (electroless plating) inner electrodes. All experiments were started with fresh metal-coated inner electrodes. The time on-stream was from the beginning of plasma formation when the high AC voltage was applied between the inner and outer electrodes.

The H₂ concentrations in the products were stable during long time runs in the tubular PACT reactors with either Pd- or Rh-coated inner electrodes, but the H₂ concentrations increased slowly in the cases of using either Ni or Au coated copper rods as inner electrodes, as shown in Fig. 3. These experimental results show that the activities for H₂O splitting in the tubular PACT reactors with different metal (Au, Ni, Rh, and Pd) coated inner electrodes are different and decreased in the order shown in Eq. [1]

$$\text{Au} > \text{Ni} > \text{Rh} > \text{Pd}. \quad [1]$$

All other experimental conditions besides the type of metal-coated inner electrode are the same.

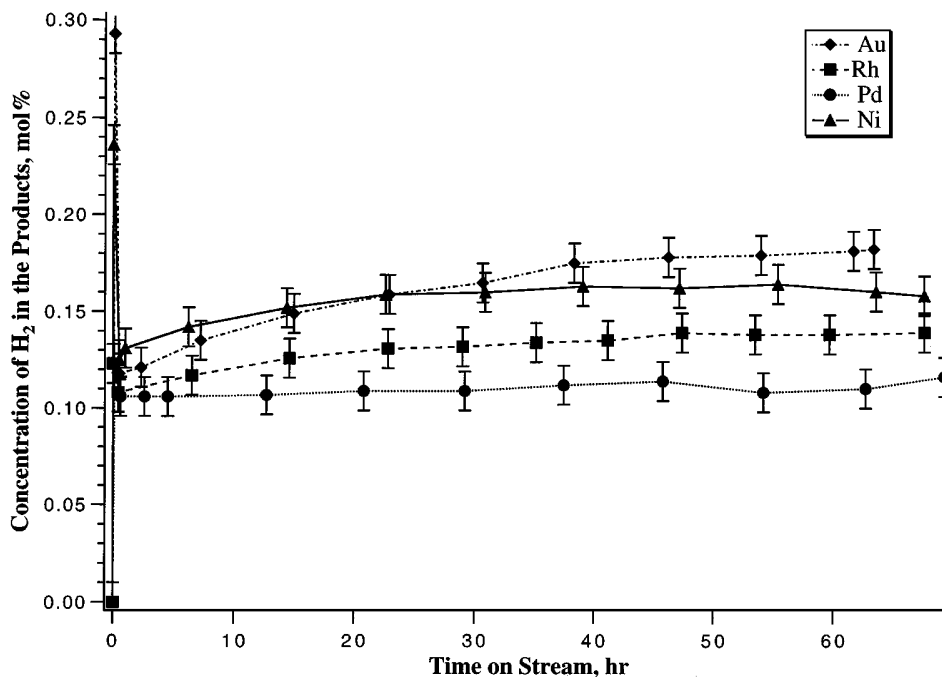


FIG. 3. H₂O splitting activity in the tubular PACT reactors with different metal coated inner electrodes. Feed: H₂O, ~2.3% in Ar; flow rate: 10 mL/min. Outer electrode: Al, 6.0 cm, grounded. Discharge gap: 0.20 mm. $V_p = 1.40$ kV; $V_{in(p-p)} = 3.3$ kV; $i = 32$ mA.

Discolorations were found on all metal-coated inner electrodes, where the plasma existed after H₂O splitting reactions. Plasmas formed in the tubular PACT reactors near the inner electrode. High activity of the inner electrodes led to more discoloration of the resultant inner electrode.

As soon as the plasma was started in the reactors, the initial hydrogen concentration in the product increased to very high values and then dropped sharply. Meanwhile, the oxygen concentration detected with GC methods was much lower, compared to the stoichiometric concentration according to the water-splitting reaction. The low oxygen concentration is due to adsorption of initially formed oxygen that reacts with the fresh inner electrodes. The rate of the reverse reaction (hydrogen reacting with oxygen to form water) was low, due to the low oxygen concentration in the gas phase. After the fresh inner electrode surface reacted with the adsorbed oxygen, the oxygen concentration increased. The rate of the reverse reaction then increased and the hydrogen concentration decreased. The initial high hydrogen yield occurs on fresh inner electrodes that have more active sites than after reaction, due to the subsequent poisoning of active sites on the inner electrodes.

Argon is the main component of the feed to the tubular PACT reactor and is probably excited initially in the plasma zone. The excited argon atoms may transfer their energy to excite water molecules into excited states during collisions with each other. The probability that water molecules are excited directly in the plasma zone is much smaller due to the much lower population of water molecules. The excited

water molecules are chemisorbed on the metal surface and are involved in catalytic dissociation reactions, leading to dissociation into hydrogen and oxygen atoms which then form hydrogen and oxygen molecules. Direct dissociation of water in the gas phase is minimal, based on comparisons with nonmetallic (glass) electrode systems. The catalytic effect of different metal-coated inner electrodes shown here also supports this energy transfer mechanism.

The used Au-coated inner electrode of the Au-tubular PACT reactor was used in further studies. Figure 4 shows the results of H₂O splitting in the tubular PACT reactors with used Au-coated inner electrodes, compared to the results for the case of fresh Au-coated inner electrodes. The used Au-coated inner electrodes presented significantly higher H₂O splitting activity than fresh Au-coated inner electrodes. This suggests that the first use of the fresh Au-coated inner electrode in H₂O splitting by plasma served as a beneficial pretreatment for the Au-coated inner electrode.

Effects of different peak voltages (V_p) on H₂O splitting by plasmas were studied with used Au-coated inner electrodes of Au-tubular PACT reactors. These results are summarized in Table 1. When V_p increases, the input voltage $V_{in(p-p)}$ and the gap current (i) through the inner and outer electrodes also increase. H₂O splitting activity increases when V_p increases from 1.20 kV to 2.50 kV, as shown by the increase of H₂ concentration in the product. When V_p was increased further to 3.00 kV, the H₂ concentration was almost as high as that when V_p was 2.50 kV. This suggests

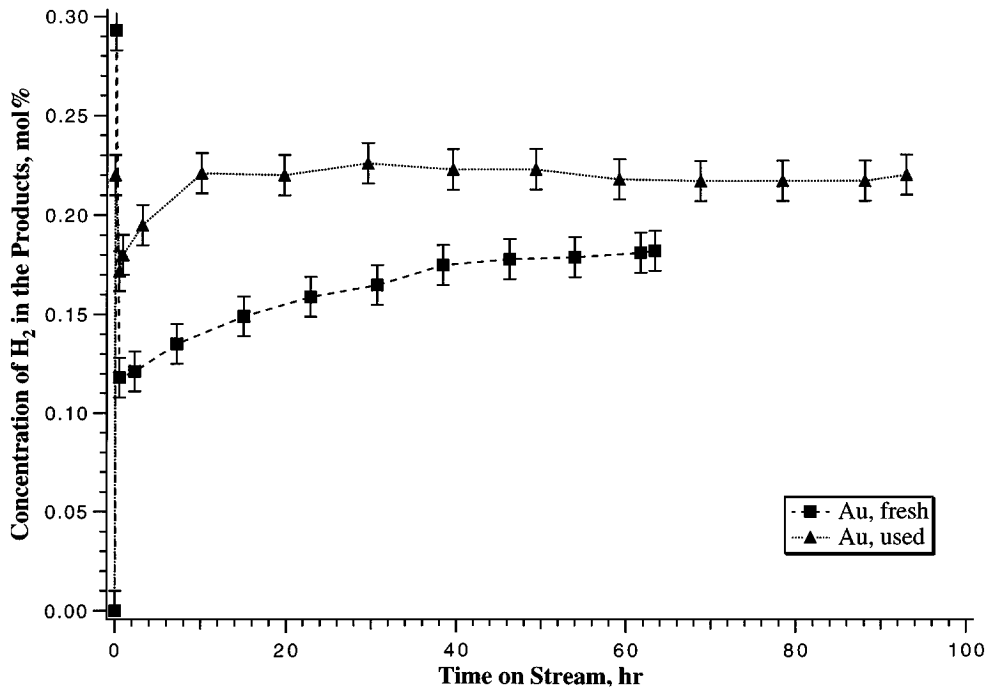


FIG. 4. H₂O splitting activity in the tubular PACT reactors with fresh and used Au-coated inner electrodes. Feed: H₂O, ~2.3% in Ar; flow rate: 10 mL/min. Outer electrode: Al, 6.0 cm, grounded. Discharge gap: 0.20 mm. $V_p = 1.40$ kV; $V_{in(p-p)} = 3.3$ kV; $i = 32$ mA.

that a certain optimal high V_p is needed to achieve significant H₂O splitting activity in Au-tubular PACT reactors.

Theoretically, the complete decomposition of 2.3% water in an argon mixture flowing at 10 mL/min requires 0.033 W of power. The power consumed during the above operating conditions was 1.59 W when V_p is at 2.50 kV and 2.17 W at 3.00 kV. For complete (100%) conversion the theoretical reactor efficiency for the optimum conditions would be 2.07% when V_p is at 2.50 kV and 1.52% at 3.00 kV. The actual conversions were both approximately 14.2%, corresponding to 0.32 mol% H₂ concentration in the product stream, which required 0.0047 W of power. Therefore, the actual efficiencies for these conditions were 0.29% when V_p is at 2.50 kV and 0.22% at 3.00 kV.

TABLE 1

Effect of the Peak Voltage V_p for H₂O Splitting in Au-Tubular PACT Reactor^a

V_p (kV)	$V_{in(p-p)}$ (kV)	i (mA)	H ₂ in products, mol%
1.20	2.8	20	0.09
1.40	3.3	32	0.21
1.80	4.3	40	0.29
2.50	5.9	45	0.32
3.00	>6.8	48	0.33

^a Feed: H₂O, ~2.3% in Ar; Flow rate: 10 mL/min. Inner electrode: Au; outer electrode: Al, 6.0 cm, grounded; discharge gap: 0.20 mm.

Although the efficiency of this process is low it has advantages over other processes in that the reaction occurs at room temperature and atmospheric pressure. There are still other variables that can be changed to further improve the efficiency of this process including flow rate, water concentration, and different carrier gases. The circuit design and power supply frequency are other variables that can influence the reaction efficiency.

B. OES: Theoretical Background

The electron temperature (T_e) is a central diagnostic parameter for plasmas. Usually, the excitation temperature is also associated with the kinetic temperature of the electrons, since excitation processes are mostly caused by electrons. OES has been used for determining the excitation temperatures. This parameter is frequently applied in high electron density plasmas using concepts derived from the local thermodynamic equilibrium (LTE) approximation. In LTE the atomic-state distribution function follows the Saha-Boltzmann equation [2] which predicts the relative direct excitation of the lower excited state,

$$n_i = \frac{N g_i \exp -(E_i/kT)}{Z}, \quad [2]$$

where n_i is the number of atoms in the i th energy state E_i , N is the total number of atoms, Z is the partition function, g_i is the statistical weight of state i usually called degeneracy; k is the Boltzmann constant; and T is the absolute temperature.

The radiant intensity I_i is given by

$$I_i = \frac{A_i g_i h c v_i}{4\pi}, \quad [3]$$

where A_i is the transition probability; h is Plank's constant; c is the speed of light; v_i is the wavenumber of the transition; and n_i is the number of atoms in the i th state. Equation [3] can be rearranged to yield

$$\ln \frac{I_{\text{obs}}}{A_i n_i g_i} = \ln \frac{h c N}{4\pi Z} - \frac{E_i}{kT}. \quad [4]$$

Consequently a graph of $\ln(I_{\text{obs}}/A_i v_i g_i)$ vs E_i should be linear with a slope of $1/kT$.

C. OES: Results and Discussion

The observed emission intensities (I_{obs}) were measured, integrated, and corrected with instrumental response factors. The wavelength (λ), the statistical weight of the transition upper level (g_i), and the spontaneous transition probability A_i were used to obtain $1/kT_{\text{exc}}$ from the slope of the fitted Boltzmann plot.

The excitation temperature is a pseudo-temperature which has to be estimated and carefully used. The spectroscopic data for several Ar and He lines were used to generate linear Boltzmann plots. The relative intensities of atomic emission lines confirm a Boltzmann distribu-

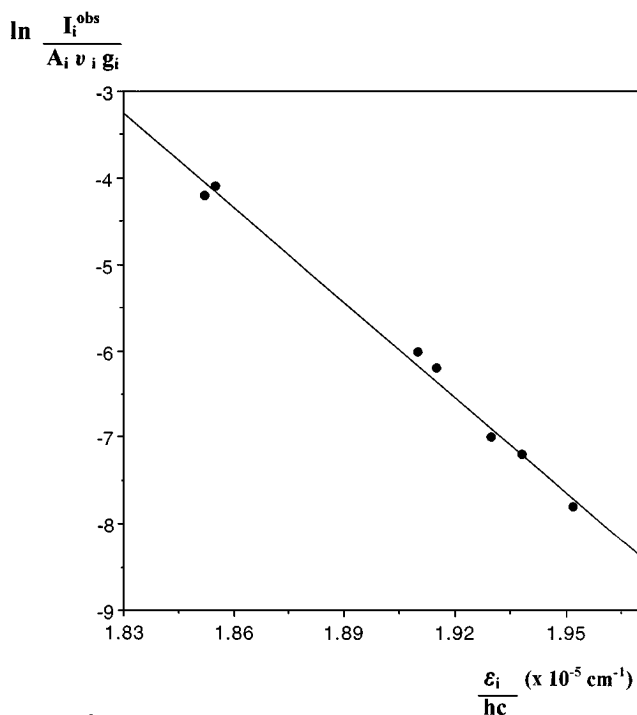


FIG. 5. Boltzmann distribution plot using atomic helium transitions for Ar + 1% He mixture at $P = 1$ atm, $V_p = 5.9$ kV, and Au as inner electrode.

tion with an excitation temperature of 4300 ± 200 K for Ar + 1% He at $V_i = 5.9$ kV using Au as an inner electrode.

Water dissociates in the plasma discharge reactors generating O, OH, and H. There are four possible ways to split water molecules: (1) by direct electron impact; (2) by energy transfer from Ar^* , (3) by electron transfer to Ar^+ and/or Ar_2^+ ; and (4) by a combination of 1, 2, and 3.

We were able to observe Ar^* emissions of Ar(I) = 696.5, 706.7, 738.4, 750.4, 763.5, 772.4, 794.8, 800.6, 801.4, and 811.5 nm; and Ar(II) 396.8, 397.9, 480.6, 506.2 nm which are drastically quenched by water during reaction. Also OH (308.9 nm), O^* (844.6 nm), H_α (656.3 nm), and H_β (486.1 nm) were weakly observed.

The O^* (844.5 nm)/ Ar^* (750.4 nm) emission intensity ratio can be used to monitor the O^* metal interaction (15). This ratio was also used for quantitative analysis of the oxygen radical.

The O^*/Ar^* emission intensity ratio depends on the metal and follows this tendency:

$$\text{O}^*/\text{Ar}^*: \text{Ni} > \text{Pd} > \text{Rh} > \text{Au} \quad [5]$$

and the corresponding excitation temperatures were

$$T_{\text{exc}}: \text{Au} > \text{Ni} > \text{Pd} > \text{Rh}. \quad [6]$$

Metal	T_{exc} (K)
Au	4300
Ni	4000
Rh	3200
Pd	3800

Note. $V_i = 5.9$ kV, $T_{\text{exc}}(\text{Ar} + 1\% \text{He}) \pm 200$ K.

We believe a complex combination of mechanisms are playing important roles in the water-splitting reaction, where surface and gas phase reactions both occur. The use of excitation temperatures as a diagnostic parameter with an OES suggests that metal/rare gas interactions may play an important role in the splitting of water via plasma chemical processes.

IV. CONCLUSIONS

In summary, significant activity for H_2O splitting by atmospheric dielectric barrier discharges has been achieved with tubular PACT reactors. Further studies are being carried out to determine the combined effects of different experimental parameters, such as different inner and outer electrodes, the lengths of outer electrodes, the discharge gaps between the inner electrode and the inner side of the quartz reactor tube, and different power supplies with different frequencies. Ultimately, the mechanism of H_2O splitting will be studied by more detailed detection of species in

the plasma zone by using optical emission spectroscopy with charge coupled detectors (CCD) in order to optimize the activity of H₂O splitting in tubular PACT reactors. Highly correlated quantum-chemical *ab initio* calculations are currently in progress in order to understand the metal/carrier gas interactions.

ACKNOWLEDGMENTS

We acknowledge the University of Connecticut, Fujitsu Limited, Hokushin Corporation, and Honda R.&D. Co., Ltd. for support of this research. We also thank Professor K. Itoyama for helpful discussions.

REFERENCES

1. Thomas, N. C., *Sci. Prog.* **72**, 32 (1988).
2. Czuppon, T. A., Knez, S. A., and Newsome, D. S., in "Encyclopedia of Chemical Technology," 4th ed. (Kirk-Othmer, Ed.), Vol. 13, p. 867. Wiley, New York, 1991.
3. Amouyal, E., *Sol. Energy Mater. Sol. Cells* **94**, 8028 (1995).
4. Bolton, J. R., *Solar Energy* **57**, 37 (1996).
5. Bard, A. J., and Fox, M. A., *Acc. Chem. Res.* **28**, 141 (1995).
6. Badyal, J. P. S., *Topics Catal.* **3**, 255 (1996).
7. Kizling, M. B., and Järäs, S. G., *Appl. Catal. A: General* **147**, 1 (1996).
8. Fridman, A. A., and Rusanov, V. D., *Pure & Appl. Chem.* **56**, 1267 (1994).
9. Miller, G. P., and Baird, J. K., *J. Phys. Chem.* **97**, 10984 (1993).
10. Venugopalan, M., and Veprek, S., in "Plasma Chemistry IV," (S. Veprek and M. Venugopalan, Eds.), Vol. 107, p. 9. Springer-Verlag, Berlin, 1983.
11. Chang, M. B., and Tseng, T. D., *J. Environ. Engrg.* **122**, 41 (1996).
12. Huang, J., and Suib, S. L., *J. Phys. Chem.* **97**, 9403 (1993).
13. Suib, S. L., and Zerger, R. P., *J. Catal.* **139**, 383 (1993).
14. Hayashi, Y., and Wakatsuki, N., 1995.
15. Inomata, K., and Oikawa, S., *Appl. Phys. Lett.* **66**, 2188 (1995).